

The BiomolBiomed publishes an “Advanced Online” manuscript format as a free service to authors in order to expedite the dissemination of scientific findings to the research community as soon as possible after acceptance following peer review and corresponding modification (where appropriate). An “Advanced Online” manuscript is published online prior to copyediting, formatting for publication and author proofreading, but is nonetheless fully citable through its Digital Object Identifier (doi®). Nevertheless, this “Advanced Online” version is NOT the final version of the manuscript. When the final version of this paper is published within a definitive issue of the journal with copyediting, full pagination, etc., the new final version will be accessible through the same doi and this “Advanced Online” version of the paper will disappear.

**RESEARCH ARTICLE****Wang et al: PANoptosis genes predict PCa outcomes****Integrative PANoptosis gene profiling  
reveals prognostic and therapeutic insights  
in prostate cancer****Yi Wang<sup>1,2#</sup>, Yiheng Du<sup>2#</sup>, Xizhi Wang<sup>2</sup>, Jiang Yu<sup>2</sup>, Qing Gu<sup>2</sup>, Guangquan Yuan<sup>2</sup>,  
Yifei Zhu<sup>2</sup>,  
Liyang Gu<sup>2</sup>, Jun Ouyang<sup>1\*</sup>**

<sup>1</sup>Department of Urology, The First Affiliated Hospital of Soochow University, Suzhou, China;

<sup>2</sup>Department of Urology, Suzhou Kowloon Hospital, Shanghai Jiao Tong University School of Medicine, Suzhou, China.

\*Correspondence to **Jun Ouyang**: [dr\\_ouyangjun@126.com](mailto:dr_ouyangjun@126.com)

# **Yi Wang** and **Yiheng Du** contributed equally to this work.

DOI: <https://doi.org/10.17305/bb.2025.11998>

## **ABSTRACT**

Prostate cancer (PCa) remains a significant global health challenge, representing the most common solid tumor in men and the fifth leading cause of cancer-related death. Despite therapeutic advances, achieving a definitive cure remains difficult. Early diagnosis and personalized treatment strategies are crucial for improving patient outcomes. Programmed cell death—particularly PANoptosis, an inflammatory pathway that integrates pyroptosis, apoptosis, and necroptosis—has emerged as a promising therapeutic target in oncology. In this study, individuals with PCa were categorized into PANoptosis-high and PANoptosis-low subgroups based on the expression levels of 45 PANoptosis-related genes. Differential gene expression analysis and subsequent enrichment analyses were conducted to explore the biological pathways associated with each subgroup. A four-gene risk signature (CASP7, ADAR, DNMI1, and NAIP) was identified, showing strong predictive value for overall survival (OS) in both training and validation cohorts. This signature was independently associated with OS and showed meaningful correlations with the tumor microenvironment, particularly immune cell infiltration and immunotherapy responsiveness. These findings suggest that the PANoptosis-related gene signature may serve as a valuable prognostic biomarker and inform immunotherapeutic strategies in PCa management.

**Keywords:** Gene risk signature; Prostate cancer; PCa; Programmed cell death.

## INTRODUCTION

Prostate cancer (PCa) is recognized as the most prevalent solid tumor among men and stands as the fifth leading contributor to cancer-related mortality on a global scale, representing a major public health concern. Genetic predisposition and environmental exposures influence the likelihood of developing PCa, with factors such as advanced age and familial history serving pivotal functions [1-3]. Patients frequently exhibit nonspecific clinical manifestations, including reduced urine flow, urgency, increased nocturia, and a sensation of incomplete bladder emptying, which often result in delayed diagnosis and elevated mortality rates [4, 5]. Although substantial progress has been made in radiotherapy, targeted therapies, and immunotherapy, attaining a definitive cure continues to present significant challenges. The early identification of individuals at an elevated risk of recurrence, coupled with prompt therapeutic intervention, can extend survival and enhance quality of life. Thus, developing reliable prognostic biomarkers to facilitate precision medicine, particularly in guiding personalized chemotherapy and immunotherapeutic strategies, remains imperative.

Programmed cell death, encompassing pyroptosis, apoptosis, and necroptosis, is fundamental in preserving homeostasis and influencing disease progression. The emergence of PANoptosis, an inflammatory programmed cell death pathway orchestrated by the PANoptosome complex, is distinguished by its integration of pyroptotic, apoptotic, and/or necroptotic features [6-10]. This phenomenon has been associated with a spectrum of pathological conditions and has garnered substantial attention in cancer research. Evidence indicates that PANoptosis serves a function in multiple cancer-related biological processes, including tumorigenesis and resistance to chemotherapy in colorectal cancer, as well as modulating the response to immunotherapy in gastric cancer [11-16]. Prior studies have demonstrated that the combination of TNF- $\alpha$  and IFN- $\gamma$  exhibits efficacy in targeting various tumor cell types, underscoring its potential clinical applications. The cooperative interaction between TNF- $\alpha$  and IFN- $\gamma$  has been shown to activate multiple signal transduction pathways, including GSDMD, GSDME, caspase-8, and MLKL. The activation of PANoptosis in tumor cells via this mechanism has been recognized as a pivotal process in suppressing

tumor initiation and restricting tumor progression, presenting opportunities for targeted therapeutic interventions [17-19]. Nevertheless, PANoptosis does not exclusively exert anti-tumor effects; in certain contexts, it may contribute to tumor progression. For instance, elevated caspase-8 levels within the nuclei of tumor cells have been reported to inhibit intrinsic apoptotic pathways while simultaneously promoting mitotic activity, thereby facilitating tumor development. Conversely, caspase-8 has also been identified as a downstream effector of granzyme, particularly facilitating GSDME cleavage and triggering pyroptosis, which enhances anti-tumor immune responses and impedes tumor proliferation [20]. Thus, further investigation into the function of PANoptosis in tumor biology holds substantial promise for clinical advancements.

This study is designed to elucidate the fundamental molecular mechanisms underlying PANoptosis-related genes (PRGs) in PCa. A systematic analysis of their expression patterns will be executed utilizing data from The Cancer Genome Atlas (TCGA) and Gene Expression Omnibus (GEO) datasets to identify PRGs that correlate with PCa prognosis. Through the development of prognostic models, insights into the tumor microenvironment (TME) status will be explored, along with predictions regarding patient responsiveness to immunotherapy. The findings are expected to assist in discovering novel prognostic biomarkers and treatment targets for PCa.

## **METHODS AND MATERIALS**

### **Data sources**

The datasets and samples related to PCa utilized in this study were acquired from multiple publicly available repositories. For the training cohort, RNA-seq data from 544 PCa patients were retrieved from the TCGA database (accessible at <https://portal.gdc.cancer.gov/>). The raw read counts underwent conversion into transcripts per kilobase million values. Furthermore, DNA methylation profiles and genetic mutation data were obtained from the cBioPortal. Information on clinicopathological characteristics and overall survival (OS) was accessed via the UCSC Xena browser (<https://xenabrowser.net/datapages/>).

An external validation set was constructed utilizing the gene expression profiling

dataset GSE70770, which comprises 203 PCa samples along with their corresponding clinical data. This dataset was acquired from the GEO database (accession number: GSE70770; <https://www.ncbi.nlm.nih.gov/geo/query/acc.cgi?acc=GSE70770>) [21, 22]. The microarray data obtained from GSE70770 underwent log<sub>2</sub> normalization.

### **Collection of PANoptosis-related genes and development of protein-protein interaction (PPI) network**

The profiles of PRGs (Table S1) were obtained from previously published studies [23, 24]. To investigate the interactions among PANoptosis-related genes, the STRING database (<https://cn.string-db.org/>) was employed for PPI network analysis [25].

### **Consensus clustering**

To classify molecular subtypes associated with PANoptosis-related genes, unsupervised consensus clustering was conducted using the “ConsensusClusterPlus” package in R [26]. This analysis was performed utilizing the expression profiles of these genes in PCa specimens. To identify the most suitable number of clusters, various cluster sizes ranging from  $k = 2$  to  $k = 10$  were assessed, with the consensus clustering procedure repeated 1,000 times to enhance result stability and accuracy. The optimal clustering parameter was systematically evaluated using the cumulative distribution function (CDF) curve, the consensus matrix, and a consistency score exceeding 0.9. Additionally, the “pheatmap” function in R was applied to depict the clustering outcomes in a heatmap format.

### **Identification of differentially expressed genes (DEGs)**

To identify DEGs in the TCGA cohort, patients were split into two cohorts based on PRG expression levels: PANoptosis-high and PANoptosis-low. Differential gene expression analysis between these cohorts was executed utilizing the “DESeq2” package in R software (version 4.0.2) [27]. Genes exhibiting an adjusted  $P$ -value of  $< 0.05$  and an absolute log<sub>2</sub> fold change exceeding 1 were regarded as markedly differentially expressed. To minimize false-positive results, adjusted  $P$ -values were applied, ensuring a more reliable selection of DEGs.

### **Enrichment analysis**

To explore the biological functions of DEGs identified between the PRGs-high and PRGs-low cohorts, Gene Ontology (GO) and Kyoto Encyclopedia of Genes and

Genomes (KEGG) enrichment analyses were executed [28, 29]. The “clusterProfiler” package in R assessed GO terms and KEGG pathways [30]. GO annotations encompassed molecular functions, biological processes, and cellular components, while KEGG enrichment analysis aimed to elucidate higher-level insights into gene function and signaling pathways. The GO and KEGG pathway examinations were executed utilizing corrected  $P$ -values  $< 0.05$  as the cutoff for statistical significance. Additionally, Gene Set Enrichment Analysis (GSEA) was executed employing GSEA software (<http://www.broadinstitute.org/gsea/index.jsp>), with a focus on the Molecular Signatures Database collection, specifically `c5.go.bp.v2023.2.Hs.symbols.gmt` [31].

### **Tumor immune analysis**

The CIBERSORT algorithm (<https://cibersort.stanford.edu/>) was employed to evaluate the composition of the tumor immune microenvironment. Expression data from PCa samples were input into CIBERSORT, and the algorithm was executed with 1,000 permutations to compute the comparative distributions of 22 distinct immune cell types [32]. The distributions of these immune cell populations in the PRGs-high and PRGs-low subgroups were determined and represented as a landscape map. Subsequently, the ESTIMATE algorithm was applied to further characterize the TME by calculating tumor purity and the immune score, facilitating a systematic pan-cancer assessment of tumor purity [33]. Furthermore, the Tumor Immune Dysfunction and Exclusion (TIDE) algorithm was applied to generate TIDE scores and predict responses to immunotherapy [34].

### **Somatic mutation analysis**

To investigate somatic mutations in PCa samples, mutation data in “maf” format were acquired from the TCGA Genomic Data Commons Data Portal. The “maftools” package in R software generated waterfall plots, comprehensively depicting the mutation landscape [35].

### **Survival analysis**

Kaplan-Meier (KM) survival curves were constructed utilizing the survival and survminer packages in R to visually compare survival distributions among different patient cohorts. Log-rank tests were applied to evaluate variations in survival

distributions between these cohorts. A *p*-value below 0.05 was regarded as statistically significant. Univariate Cox proportional hazards regression analysis was conducted to examine the relationship between risk scores and OS status, with variables displaying a *p*-value under 0.05 deemed significant and selected for multivariate analysis. To determine whether the variables identified in the univariate analysis remained significant after adjusting for possible confounders, a subsequent multivariate Cox proportional hazards regression model was conducted.

### **Screening of prognosis-related signatures**

Prognosis-related PRGs were ascertained through univariate Cox regression analysis. Statistically significant genes were selected as candidate inputs for further modeling. Subsequently, Lasso Cox regression analysis was executed utilizing the 'glmnet' package in R to compute precise coefficient values. Based on these selected genes, a multivariate Cox model was developed [36].

### **Cell culture and transient transfection**

The cell lines RWPE-1, PC-3M, 22RV1, C4-2, DU145, and PC-3 were procured from Beijing Bena Biotechnology Co. (Beijing, China). These cells were kept in a DMEM/F-12 medium comprising 10% FBS (Gibco). Transfection of the negative control (NC) and ADAR-targeting siRNA (Sagon, China) was performed using Lipofectamine 2000 (Invitrogen, Thermo Fisher, USA).

### **Quantitative real-time polymerase chain reaction (qRT-PCR)**

Total RNA isolation was executed utilizing TRIzol reagent (Thermo Fisher, USA). Real-time PCR analysis was executed employing FastStart Universal SYBR Green Master on RNA specimens (2 µg) via the LightCycler 480 PCR System (Roche, USA). The amplification mixture (20 µl) contained cDNA as a template, comprising 2 µl of cDNA sample, 10 µl of PCR solution, 0.5 µl of both forward and reverse primers, plus the required amount of water. The thermal cycling protocol involved initial denaturation at 95 °C for 30 s, succeeded by 45 rounds of 94 °C for 15 s, 56 °C for 30 s, and 72 °C for 20 s. Triple independent replicates were executed for each specimen. The threshold cycle (CT) values were determined and standardized to GAPDH expression per sample, applying the  $2^{-\Delta\Delta CT}$  methodology. The relative mRNA levels were subsequently

evaluated against normal tissue controls. The primer sequences employed for target genes are listed below:

#### **Determination of 5-ethynyl-2'-deoxyuridine (EdU)**

The EdU assay employed the BeyoClick™ EdU Cell Proliferation Kit with Alexa Fluor 594 (Biotek, Shanghai, China). Following PBS rinsing, cells underwent EdU solution treatment for 2 h, after which nuclear staining was performed using DAPI solution. Subsequently, after additional washing steps, the specimens were examined under an inverted microscope (Olympus).

#### **Drug treatment**

Docetaxel was procured from MedChemExpress (MCE, HY-B0011), dissolved in DMSO, and subsequently introduced into the medium at the specified concentration.

#### **Cell viability**

Cell viability was assessed utilizing the Cell Counting Kit-8 assay (Beyotime, China) per the supplier's protocols. Cells subjected to various treatments were placed into 96-well plates at  $1 \times 10^3$  cells per well. The CCK-8 solution was introduced at the designated time points. After a 2-hour incubation at 37 °C, the optical density at 450 nm for each well was ascertained utilizing a microplate reader (BioTeK, USA).

#### **Immunofluorescence**

The medium was procured from PC-3M and 22RV1 cell lines originating from both the si-NC and si-ADAR cohorts. Following high-speed centrifugation, the supernatants were collected to prepare the conditioned medium. Subsequently, the conditioned medium was co-cultured with THP-1 (Bena Biotechnology, China)-induced macrophages to investigate the regulatory influence of PC-3M and 22RV1 on macrophage polarization before and after ADAR knockdown.

Following a 12-hour co-culture of macrophages with the conditioned medium, fixation was performed using paraformaldehyde for 10 min, succeeded by antigenic blocking with QuickBlock™ solution (Beyotime, P0220). Subsequently, incubation was conducted overnight at 4 °C with the designated primary antibodies: CD86 Polyclonal antibody (Proteintech, 13395-1-AP) and CD206 Monoclonal antibody (Proteintech, 60143-1-Ig). After incubation of the primary antibody for 2 h at room temperature with the corresponding fluorescent secondary antibody, immunofluorescence images were

captured using a Leica DM2500 microscope.

### **Statistical analysis**

All statistical analyses were performed utilizing R software (version 4.3.3) and GraphPad Prism 8. For comparisons between two cohorts with a normally distributed variable, an unpaired Student's t-test was applied to ascertain statistical differences. When the variable did not conform to a normal distribution, the Mann-Whitney U test was applied to assess statistical significance between the two cohorts. In multi-group comparisons, parametric methods (e.g., one-way ANOVA) or non-parametric approaches (e.g., Kruskal-Wallis test) were utilized for analysis. Additionally, KM survival analysis was carried out to investigate the OS variations between high-risk and low-risk cohorts, utilizing log-rank tests for survival distribution assessment. Additionally, the ROC curve was constructed, and the AUC metric was calculated to evaluate the risk score's predictive performance. Statistical significance was established at  $p < 0.05$ .

## **RESULTS**

### **PANoptosis-related subtypes clustering**

A total of 45 PRGs were identified based on previous studies. A PPI network analysis was conducted utilizing the STRING database to uncover the interconnections among these genes (**Figure 1A**). Additionally, the distribution profiles of these genes were examined in both normal and PCa tissues. The findings indicated that most PRGs, including BAX, NFS1, GSDMA, CDK1, GSDMB, DIABLO, and CASP8, exhibited significant upregulation in PCa samples (**Figure 1B**). Furthermore, PANoptosis-associated clusters in PCa were identified through consensus clustering. By implementing k-means clustering on the TCGA cohort, two clusters with distinct PRG expression patterns were distinguished (**Figures 1D, E**). Notably, cluster C2 demonstrated elevated PRG expression levels, classifying it as the PANoptosis-high subtype, whereas cluster C1 was characterized by lower expression levels, defining it as the PANoptosis-low subtype (**Figure 1F**). Survival analysis revealed notable differences in clinical outcomes between these subtypes, with the PANoptosis-low

subtype being linked to an unfavorable prognosis, whereas the PANoptosis-high subtype exhibited better clinical results ([Figure 1G](#)).

### **DEGs and enriched pathways in PANoptosis subtypes**

Considering that the PANoptosis-high subtype was linked to favorable clinical outcomes, whereas the PANoptosis-low subtype was associated with a unfavorable prognosis, an investigation was conducted to identify key DEGs and signaling pathways in each subtype to elucidate the molecular mechanisms influencing prognosis. The analysis identified 746 DEGs ([Figures 2A, B](#)), encompassing 617 upregulated and 129 downregulated genes.

GO enrichment analysis demonstrated that elevated genes within the PANoptosis-high subtype were predominantly involved in immune-related biological processes, encompassing cytokine production enhancement, lymphocyte differentiation, leukocyte-mediated immunity, and immune response-regulating signaling pathways. Similarly, KEGG pathway enrichment examination suggested that these elevated genes were markedly associated with immune activity pathways, encompassing cytokine-cytokine receptor interaction, viral protein interaction with cytokine and cytokine receptors, and chemokine signaling ([Figure 2C](#)). Collectively, these findings suggest that the PANoptosis-high subtype is defined by an immune-active microenvironment, which may contribute to its more favorable clinical outcomes. To examine the activated signaling cascades within the PANoptosis-high subgroup, GSEA was conducted to compare the PANoptosis-high and PANoptosis-low cohorts. This analysis identified differential enrichment of gene sets linked to immune pathways, including granulocyte chemotaxis and the adaptive immune response ([Figure 2D](#)).

### **Somatic mutations and TME in PANoptosis subtypes**

Distinct somatic mutation profiles were identified across the subtypes ([Figures 3A, B](#)). Although TP53, TTN, SPOP, MUC16, and SYNE1 emerged as the genes with the highest mutation rates, their mutation frequencies differed between subtypes. Notably, the PANoptosis-high subtype demonstrated a higher prevalence of TP53 and TTN mutations, comprising 14% and 11% of total mutations, respectively, in contrast to 9%

and 10% observed in the PANoptosis-low subtype. Growing research indicates that PANoptosis is vital in eliciting anti-tumor immune responses. This investigation analyzed the TME configuration concerning PANoptosis-high and PANoptosis-low classifications. The analysis revealed that immune scores exhibited markedly elevated levels, while tumor purity showed notably reduced levels in the PANoptosis-high category relative to the PANoptosis-low cohort ([Figure 4A](#)). The investigation further explored variations in immune cell infiltration across 22 immune cell populations between these classifications utilizing the CIBERSORT methodology combined with the LM22 signature matrix. The outcomes procured from examining 544 PCa cases within the TCGA database are depicted in [Figure 4B](#). Notably, patients classified under the PANoptosis-high subtype demonstrated a substantially increased presence of memory B cells, resting dendritic cells, M1 macrophages, activated mast cells, neutrophils, activated memory CD4+ T cells, resting memory CD4+ T cells, CD8+ T cells, and  $\gamma\delta$  T cells ([Figure 4C](#)). Furthermore, all immune checkpoints exhibited upregulation in the PANoptosis-high subtype, whereas a contrasting trend was detected in the PANoptosis-low subtype ([Figure 4D](#)). This finding suggests that the PANoptosis-high subtype is linked to an immune-hot phenotype, while the PANoptosis-low subtype corresponds to an immune-cold phenotype.

### **Development and verification of the PANoptosis risk signature**

A prognostic model was developed based on PRGs. In the Cox univariate analysis, four PRGs were identified as being markedly linked to the OS of patients ([Figure 5A](#)). Moreover, these four PRGs were selected and validated for inclusion in the prediction model using LASSO regression analysis ([Figure 5B](#)). The risk score model was formulated using the following equation: Risk score =  $(0.9075)*CASP7 + (0.0645)*ADAR + (0.6644)*DNM1L + (1.1522)*NAIP$ . Additionally, the correlation between survival status and risk score was investigated. These observations indicated that the proportion of surviving patients in the low-risk cohort was markedly elevated versus the high-risk cohort ([Figure 5C](#)). The prognostic relevance of this risk profile in PCa was further assessed through KM analysis ([Figure 5D](#)). Within the TCGA cohort,

a high-risk score was linked to poorer OS, with these outcomes being validated in the GEO dataset ([Figure 5E](#)).

### **Connection between PANoptosis risk signature and TME**

The TIDE tool was employed to assess the predictive potential of the PANoptosis risk signature in determining the clinical efficacy of immunotherapy. The findings indicated that patients classified in the immunotherapy non-response cohort exhibited higher PANoptosis risk scores, suggesting that those with lower risk scores might derive greater benefit from immunotherapy ([Figure 6A](#)). Considering PANoptosis's crucial immunological function in anti-tumor immune responses, an in-depth analysis was executed to investigate the association between the PANoptosis risk score and the TME. The outcomes demonstrated that an elevated risk score was negatively associated with resting dendritic cells ([Figure 6B](#)). Additionally, in the GEO cohort, a negative correlation was observed between an increased risk score and both Macrophages M1 and Macrophages M2 ([Figure 6C](#)). Univariate and multivariate Cox analyses were executed to assess the independent prognostic significance of the PANoptosis risk signature. The univariate Cox analysis identified a high PANoptosis risk score as markedly linked to diminished OS ([Figure 6D](#)). Moreover, multivariate Cox analysis confirmed the PANoptosis risk score's capability to function as an independent prognostic factor for individuals with PCa ([Figure 6E](#)).

### **ADAR promotes PCa progression *in vitro***

To validate the bioinformatics model, CASP7, ADAR, DNMI1L, and NAIP transcript levels were analyzed in PCa cell lines. Compared to RWPE-1, transcripts of CASP7, ADAR, DNMI1L, and NAIP exhibited upregulation in PC-3M and 22RV1, with ADAR demonstrating the most pronounced increase ([Figure 7A-D](#)). Furthermore, ADAR transcript levels in RWPE-1 were evaluated against those in C4-2, DU145, and PC-3. ADAR was markedly upregulated in PCa cell lines C4-2, DU145, and PC-3, indicating that ADAR transcript upregulation is a widespread phenomenon in PCa cell lines ([Figure 7E](#)).

For this reason, ADAR was selected for further investigation. The inhibitory efficiency of small interfering RNAs targeting ADAR was validated in PC-3M and 22RV1. Both si-ADAR-1 and si-ADAR-2 suppressed ADAR transcription in these cell lines, with si-ADAR-2 exhibiting the most pronounced inhibitory effect. Consequently, si-ADAR-2 (si-ADAR) was chosen for subsequent experiments (Figure 7F-G). A substantial reduction in cell viability was observed after ADAR suppression in PC-3M and 22RV1 cell lines. Additionally, the IC<sub>50</sub> values of PC-3M and 22RV1 treated with Docetaxel *in vitro* were markedly decreased (Figure 7H-K).

The proliferative capacity of PC-3M and 22RV1 cell lines was markedly reduced following ADAR knockdown, as indicated by a decline in the percentage of EdU-positive cells and a reduction in clone formation (Figure 8A-D). Given that EMT serves a pivotal function in cancer metastasis, the transcription of EMT-related markers in PC-3M and 22RV1 was examined before and after ADAR knockdown. The results demonstrated that CDH1 expression was upregulated, whereas CDH2 and VIM were downregulated following ADAR silencing (Figure 8E-F), suggesting that ADAR promotes EMT in PCa cell lines. Additionally, the impact of ADAR on cellular apoptosis and pyroptosis was assessed, revealing that the transcriptional upregulation of BAX, CASP1, and GSDMD following ADAR knockdown reflects its inhibitory effect on programmed cell death (Figure 8G-H).

Finally, the regulatory influence of ADAR on the immune microenvironment was examined through its impact on macrophages, which tended to polarize toward the M1 phenotype following ADAR knockdown. This observation suggests that ADAR contributes to establishing an inflammation-suppressive TME (Figure 9A-D).

## **DISCUSSION**

Despite notable advancements in diagnostic and therapeutic methodologies, PCa continues to be a predominant contributor to cancer-related mortality in men, with recurrence occurring in up to 40% of individuals diagnosed with localized PCa within a decade [37-39]. Androgen deprivation therapy has long been recognized as a conventional approach for PCa treatment. However, a considerable proportion of

patients with advanced-stage disease inevitably progress to castration-resistant PCa [40]. In recent years, innovative treatment approaches, including immunotherapy, have been investigated to potentiate the immune system's capacity to eradicate malignant cells [41-44]. Nevertheless, the effectiveness of immunotherapy in managing PCa, as well as its implications for patient prognosis, remains a topic of ongoing debate. Certain studies indicate that the intricate TME intrinsic to PCa fosters an inherent resistance to immunotherapeutic interventions, thereby complicating the identification of efficacious treatment strategies [45-47]. Consequently, delineating subpopulations that benefit from PCa immunotherapy and establishing biomarkers predictive of patient prognosis are imperative steps toward optimizing therapeutic outcomes in PCa management.

Recent investigations have highlighted the essential role of PRGs in PCa [48-50]. These genes govern the assembly of the PANoptosome complex, which integrates the molecular mechanisms underlying pyroptosis, necroptosis, and apoptosis [7]. This unified pathway, termed PANoptosis, is pivotal in modulating tumor cell death and immune responses in PCa. Aberrant expression and notable mutations in PRGs have been identified across multiple cancer types, with numerous PRGs functioning as tumor risk determinants in diverse malignancies. These observations indicate that PANoptosis serves a crucial function in cancer development, and its induction could potentially suppress both tumor initiation and progression.[17] For instance, research performed by Jianzhong et al. demonstrates that modifications in PRG expression can substantially alter the immune microenvironment and therapeutic responsiveness in PCa [51]. Similarly, research led by Yanmei Wang and her team identified a notable connection between PANoptosis and clear cell renal cell carcinoma, further establishing a prognostic model utilizing three specific miRNAs to predict survival outcomes in cancer patients.[52] Within the scope of PRAD research, the intricate interactions and regulatory networks linked to PANoptosis have been explored, encompassing gene mutations, transcriptional alterations, methylation modifications, and their correlations with clinical characteristics.[17] Hence, this investigation sought to understand PANoptosis functionality in PCa and construct a prognostic signature founded on PRGs.

In this study, a total of 45 PRGs were compiled from previously conducted relevant research. Based on the expression profiles of these PRGs, PCa patients were categorized into two distinct PANoptosis subgroups through consensus clustering. Subsequently, differential gene expression analysis and functional enrichment analysis were executed, revealing that these genes participate in immune-associated pathways, encompassing the PI3K-Akt and TNF signaling pathways. To further delineate immune disparities between the PANoptosis-high and PANoptosis-low subgroups and to deepen the understanding of the TME's role in disease advancement and treatment outcomes, immune infiltration and TIDE analyses were conducted. The findings indicate a substantial divergence in immune phenotypes: the PANoptosis-high subgroup exhibits an immune-hot phenotype, whereas the PANoptosis-low subgroup presents an immune-cold phenotype. In individuals classified within the PANoptosis-high subgroup, an increased proportion of resting dendritic cells, M1 macrophages, and other immune cells was observed. The TME has been shown to have a significant impact on tumors.[53-56] Tumor-associated macrophages (TAMs) constitute a major immune cell population within the inflammatory TME. As heterogeneous macrophages, TAMs exhibit both pro-inflammatory (M1) and immunosuppressive (M2) functionalities [57]. M1 macrophages are pivotal in the PCa TME, characterized by their ability to secrete abundant pro-inflammatory cytokines and chemokines. These cells demonstrate an enhanced capacity for antigen presentation and complement-mediated phagocytosis, primarily functioning to eliminate pathogens and initiate Th1 immune responses while also exerting direct cytotoxic effects on both microorganisms and tumor cells. Conversely, M2 macrophages are commonly implicated in tumor immune evasion, angiogenesis, tumor proliferation, and metastasis [58]. The polarization of macrophages is a highly intricate biological process meticulously regulated by multiple factors, with its polarization state exerting a profound influence on inflammatory responses and tumor development [58]. Within the complex TME of PCa, various chemokines modulate macrophage polarization. For instance, CCL2 has been shown to enhance LPS-induced IL-10 production, while CCL2 inhibition stimulates the

manifestation of genes and cytokines associated with M1 polarization while concurrently suppressing M2 markers [59]. Additionally, research by Cristina I. Caescu and colleagues ascertained miR-21 as a molecule activated by the Y721 site (pTyr-721) of colony-stimulating factor-1 (CSF-1), which facilitates the suppression of the M1 phenotype while promoting the M2 phenotype [60]. Another critical regulatory factor, miRNA-155, exhibits significant elevation during M1 macrophage polarization and a notable reduction in M2 polarization. Enhanced expression of miRNA-155 promotes the polarization of M2 macrophages through the miR-155/SHIP1 pathway, consequently expediting tumor cell invasion, proliferation, and migration [61, 62]. Based on these findings, it is postulated that M1 macrophage infiltration may provide survival advantages for patients exhibiting high PANoptosis subtypes. Further investigation into the regulatory mechanisms governing macrophage polarization in PCa could yield novel insights and therapeutic strategies. Subsequent survival analysis identified four PRGs—CASP7, ADAR, DNMI1L, and NAIP—as being markedly associated with PCa prognosis. Cysteine aspartate-specific protease (Caspase) serves a crucial function in apoptosis and inflammatory regulation, with CASP7 (Caspase-7) being a key protease modulating these processes [63, 64]. Research by So Hee Kim et al. demonstrated that OTUD6A functions as a deubiquitinase by eliminating the K48-linked polyubiquitin chain from nucleolin and the K63-linked polyubiquitin chain from Caspase-7. Both nucleolin and Caspase-7, identified as OTUD6A substrates, have been proposed as potential therapeutic targets in cancer treatment [65]. ADAR is a core enzyme involved in RNA editing [66], with previous research indicating a strong correlation between ADAR dysregulation and tumor onset and progression. Julia Ramírez-Moya et al. found that ADAR promotes thyroid cancer development through RNA editing of CDK13 [67]. Similarly, Hao Yu et al. reported that ADAR is markedly upregulated in bladder cancer tissues and shows a strong correlation with unfavorable patient outcomes. Furthermore, ADAR has been shown to markedly enhance the proliferation, migration, and invasion of bladder cancer cells [68]. DNMI1L, a mitochondrial fission-associated protein, has emerged as a promising therapeutic candidate across various malignancies [69]. Research by Akane Inoue Yamauchi et al.

revealed that the absence of DNMI1L increases apoptosis in colon cancer cells [70]. Additionally, Qi Xie and colleagues discovered that DNMI1L depletion induces apoptosis in malignant brain tumor-initiating cells and markedly inhibits tumor growth [71]. NAIP, which belongs to the IAP family, is expressed in mammalian cells and can inhibit apoptosis triggered by diverse signals [72]. Moreover, previous studies have suggested that NAIP mediates innate immune inflammatory responses by activating caspase-1, 4, and 5 [73]. The study conducted by Yuk Kwan Chen et al. demonstrated that NAIP alleles undergo methylation in normal oral mucosal tissue, potentially representing an early oncogenic event [74]. Additionally, Jaewon Choi and his research team observed that NAIP expression is absent in normal breast tissue but is markedly elevated in breast cancer [75]. Although these genes have been extensively associated with the pathogenesis and advancement of various malignancies, their specific mechanistic roles in PCa remain to be fully elucidated. Ultimately, prognosis-associated signatures derived from PRGs exhibited strong predictive performance in OS across training, internal validation, and external validation cohorts.

Despite the promising outcomes observed, certain limitations inherent to this research must be acknowledged. Firstly, while PRG-based prognostic features have demonstrated strong predictive efficacy across both internal and external cohorts, the study predominantly relies on retrospective data, which may introduce potential biases. To confirm the clinical applicability and robustness of the proposed risk model, prospective clinical trials remain essential. Secondly, although functional enrichment analysis and immune infiltration assessments offer valuable insights into the TME and the immune disparities between PANoptosis-high and PANoptosis-low subgroups, the precise molecular mechanisms underlying these differences have yet to be fully elucidated. Addressing these limitations in future investigations will further reinforce the clinical significance of PRG and its potential role in informing PCa treatment strategies.

## **CONCLUSION**

In conclusion, a practical PANoptosis-risk algorithm based on four PRGs was

developed and validated, with the proposed signature serving as a potential prognostic model for PCa. Furthermore, this study unveiled novel perspectives regarding the connection between the PRG score and the immune microenvironment, offering essential perspectives for the application of immunotherapy in PCa patients.

**Conflict of interest:** Authros declare no conflicts of interest.

**Data availability statement:** The training set data was sourced from the TCGA database (<https://portal.gdc.cancer.gov>). Corresponding clinical information for the training cohort was retrieved from the UCSC Xena database (<https://xenabrowser.net/datapages/>). Data for the external validation set (GSE70770) was obtained from the GEO database (<https://www.ncbi.nlm.nih.gov/geo/>).

**Funding:** This investigation was funded by the Basic Research on Medical and Health Application of Suzhou Municipal Science and Technology Bureau (Grant number: SKJY2021031 and SKY2023111), the Pre-research Fund of the Suzhou Kowloon Hospital (Grant number: SZJL202201), the Medical Education Collaborative Innovation Fund of Jiangsu University (No. JDYY2023131).

**Submitted:** 06 January 2025

**Accepted:** 17 April 2025

**Published online:** 19 June 2025

## REFERENCES

1. **Prostate cancer.** *Nat Rev Dis Primers* 2021, **7**(1):8.
2. Parker C, Castro E, Fizazi K, Heidenreich A, Ost P, Procopio G, Tombal B, Gillessen S: **Prostate cancer: ESMO Clinical Practice Guidelines for diagnosis, treatment and follow-up.** *Ann Oncol* 2020, **31**(9):1119-1134.
3. Siegel DA, O'Neil ME, Richards TB, Dowling NF, Weir HK: **Prostate Cancer Incidence and Survival, by Stage and Race/Ethnicity - United States, 2001-2017.** *MMWR Morb Mortal Wkly Rep* 2020, **69**(41):1473-1480.
4. Litwin MS, Tan HJ: **The Diagnosis and Treatment of Prostate Cancer: A Review.** *Jama* 2017, **317**(24):2532-2542.
5. Nguyen-Nielsen M, Borre M: **Diagnostic and Therapeutic Strategies for Prostate Cancer.** *Semin*

- Nucl Med* 2016, **46**(6):484-490.
6. Sun X, Yang Y, Meng X, Li J, Liu X, Liu H: **PANoptosis: Mechanisms, biology, and role in disease.** *Immunol Rev* 2024, **321**(1):246-262.
  7. Zhu P, Ke ZR, Chen JX, Li SJ, Ma TL, Fan XL: **Advances in mechanism and regulation of PANoptosis: Prospects in disease treatment.** *Front Immunol* 2023, **14**:1120034.
  8. Pandian N, Kanneganti TD: **PANoptosis: A Unique Innate Immune Inflammatory Cell Death Modality.** *J Immunol* 2022, **209**(9):1625-1633.
  9. Shi C, Cao P, Wang Y, Zhang Q, Zhang D, Wang Y, Wang L, Gong Z: **PANoptosis: A Cell Death Characterized by Pyroptosis, Apoptosis, and Necroptosis.** *J Inflamm Res* 2023, **16**:1523-1532.
  10. Karati D, Kumar D: **Molecular Insight into the Apoptotic Mechanism of Cancer Cells: An Explicative Review.** *Current molecular pharmacology* 2024, **17**:e18761429273223.
  11. Qi Z, Zhu L, Wang K, Wang N: **PANoptosis: Emerging mechanisms and disease implications.** *Life Sci* 2023, **333**:122158.
  12. Ocansey DKW, Qian F, Cai P, Ocansey S, Amoah S, Qian Y, Mao F: **Current evidence and therapeutic implication of PANoptosis in cancer.** *Theranostics* 2024, **14**(2):640-661.
  13. Liu Z, Sun L, Peng X, Zhu J, Wu C, Zhu W, Huang C, Zhu Z: **PANoptosis subtypes predict prognosis and immune efficacy in gastric cancer.** *Apoptosis* 2024, **29**(5-6):799-815.
  14. Karki R, Sundaram B, Sharma BR, Lee S, Malireddi RKS, Nguyen LN, Christgen S, Zheng M, Wang Y, Samir P *et al*: **ADAR1 restricts ZBP1-mediated immune response and PANoptosis to promote tumorigenesis.** *Cell Rep* 2021, **37**(3):109858.
  15. Pan H, Pan J, Li P, Gao J: **Characterization of PANoptosis patterns predicts survival and immunotherapy response in gastric cancer.** *Clin Immunol* 2022, **238**:109019.
  16. Karki R, Sharma BR, Lee E, Banoth B, Malireddi RKS, Samir P, Tuladhar S, Mummareddy H, Burton AR, Vogel P *et al*: **Interferon regulatory factor 1 regulates PANoptosis to prevent colorectal cancer.** *JCI Insight* 2020, **5**(12).
  17. Gao J, Xiong A, Liu J, Li X, Wang J, Zhang L, Liu Y, Xiong Y, Li G, He X: **PANoptosis: bridging apoptosis, pyroptosis, and necroptosis in cancer progression and treatment.** *Cancer gene therapy* 2024, **31**(7):970-983.
  18. Malireddi RKS, Karki R, Sundaram B, Kancharana B, Lee S, Samir P, Kanneganti TD: **Inflammatory Cell Death, PANoptosis, Mediated by Cytokines in Diverse Cancer Lineages Inhibits Tumor Growth.** *ImmunoHorizons* 2021, **5**(7):568-580.
  19. Manohar SM: **At the Crossroads of TNF  $\alpha$  Signaling and Cancer.** *Current molecular pharmacology* 2024, **17**(1):e060923220758.
  20. Jiang M, Qi L, Li L, Wu Y, Song D, Li Y: **Caspase-8: A key protein of cross-talk signal way in "PANoptosis" in cancer.** *International journal of cancer* 2021, **149**(7):1408-1420.
  21. Ross-Adams H, Lamb AD, Dunning MJ, Halim S, Lindberg J, Massie CM, Egevad LA, Russell R, Ramos-Montoya A, Vowler SL *et al*: **Integration of copy number and transcriptomics provides risk stratification in prostate cancer: A discovery and validation cohort study.** *EBioMedicine* 2015, **2**(9):1133-1144.
  22. Whittington T, Gao P, Song W, Ross-Adams H, Lamb AD, Yang Y, Svezia I, Klevebring D, Mills IG, Karlsson R *et al*: **Gene regulatory mechanisms underpinning prostate cancer susceptibility.** *Nat Genet* 2016, **48**(4):387-397.
  23. Wang Y, Kanneganti TD: **From pyroptosis, apoptosis and necroptosis to PANoptosis: A mechanistic compendium of programmed cell death pathways.** *Comput Struct Biotechnol J*

- 2021, **19**:4641-4657.
24. Zheng Z, Li K, Yang Z, Wang X, Shen C, Zhang Y, Lu H, Yin Z, Sha M, Ye J *et al*: **Transcriptomic analysis reveals molecular characterization and immune landscape of PANoptosis-related genes in atherosclerosis**. *Inflamm Res* 2024, **73**(6):961-978.
  25. Szklarczyk D, Gable AL, Lyon D, Junge A, Wyder S, Huerta-Cepas J, Simonovic M, Doncheva NT, Morris JH, Bork P *et al*: **STRING v11: protein-protein association networks with increased coverage, supporting functional discovery in genome-wide experimental datasets**. *Nucleic Acids Res* 2019, **47**(D1):D607-d613.
  26. Wilkerson MD, Hayes DN: **ConsensusClusterPlus: a class discovery tool with confidence assessments and item tracking**. *Bioinformatics* 2010, **26**(12):1572-1573.
  27. Love MI, Huber W, Anders S: **Moderated estimation of fold change and dispersion for RNA-seq data with DESeq2**. *Genome Biol* 2014, **15**(12):550.
  28. **The Gene Ontology Resource: 20 years and still GOing strong**. *Nucleic Acids Res* 2019, **47**(D1):D330-d338.
  29. Kanehisa M, Goto S, Furumichi M, Tanabe M, Hirakawa M: **KEGG for representation and analysis of molecular networks involving diseases and drugs**. *Nucleic Acids Res* 2010, **38**(Database issue):D355-360.
  30. Yu G, Wang LG, Han Y, He QY: **clusterProfiler: an R package for comparing biological themes among gene clusters**. *Omics* 2012, **16**(5):284-287.
  31. Subramanian A, Tamayo P, Mootha VK, Mukherjee S, Ebert BL, Gillette MA, Paulovich A, Pomeroy SL, Golub TR, Lander ES *et al*: **Gene set enrichment analysis: a knowledge-based approach for interpreting genome-wide expression profiles**. *Proc Natl Acad Sci U S A* 2005, **102**(43):15545-15550.
  32. Newman AM, Steen CB, Liu CL, Gentles AJ, Chaudhuri AA, Scherer F, Khodadoust MS, Esfahani MS, Luca BA, Steiner D *et al*: **Determining cell type abundance and expression from bulk tissues with digital cytometry**. *Nat Biotechnol* 2019, **37**(7):773-782.
  33. Aran D, Sirota M, Butte AJ: **Systematic pan-cancer analysis of tumour purity**. *Nat Commun* 2015, **6**:8971.
  34. Jiang P, Gu S, Pan D, Fu J, Sahu A, Hu X, Li Z, Traugh N, Bu X, Li B *et al*: **Signatures of T cell dysfunction and exclusion predict cancer immunotherapy response**. *Nat Med* 2018, **24**(10):1550-1558.
  35. Mayakonda A, Lin DC, Assenov Y, Plass C, Koeffler HP: **Maftools: efficient and comprehensive analysis of somatic variants in cancer**. *Genome Res* 2018, **28**(11):1747-1756.
  36. Engebretsen S, Bohlin J: **Statistical predictions with glmnet**. *Clinical epigenetics* 2019, **11**(1):123.
  37. Tourinho-Barbosa R, Srougi V, Nunes-Silva I, Baghdadi M, Rembeyo G, Eiffel SS, Barret E, Rozet F, Galiano M, Cathelineau X *et al*: **Biochemical recurrence after radical prostatectomy: what does it mean?** *Int Braz J Urol* 2018, **44**(1):14-21.
  38. Shore ND, Moul JW, Pienta KJ, Czernin J, King MT, Freedland SJ: **Biochemical recurrence in patients with prostate cancer after primary definitive therapy: treatment based on risk stratification**. *Prostate Cancer Prostatic Dis* 2024, **27**(2):192-201.
  39. Boyle P, Severi G, Giles GG: **The epidemiology of prostate cancer**. *Urol Clin North Am* 2003, **30**(2):209-217.
  40. Narayan V, Ross AE, Parikh RB, Nohria A, Morgans AK: **How to Treat Prostate Cancer With**

- Androgen Deprivation and Minimize Cardiovascular Risk: A Therapeutic Tigtrope.** *JACC CardioOncol* 2021, **3**(5):737-741.
41. Hong WX, Haebe S, Lee AS, Westphalen CB, Norton JA, Jiang W, Levy R: **Intratumoral Immunotherapy for Early-stage Solid Tumors.** *Clin Cancer Res* 2020, **26**(13):3091-3099.
  42. Szeto GL, Finley SD: **Integrative Approaches to Cancer Immunotherapy.** *Trends Cancer* 2019, **5**(7):400-410.
  43. Lefler DS, Manobianco SA, Bashir B: **Immunotherapy resistance in solid tumors: mechanisms and potential solutions.** *Cancer Biol Ther* 2024, **25**(1):2315655.
  44. Cha JH, Chan LC, Song MS, Hung MC: **New Approaches on Cancer Immunotherapy.** *Cold Spring Harb Perspect Med* 2020, **10**(8).
  45. Wang I, Song L, Wang BY, Rezazadeh Kalebasty A, Uchio E, Zi X: **Prostate cancer immunotherapy: a review of recent advancements with novel treatment methods and efficacy.** *Am J Clin Exp Urol* 2022, **10**(4):210-233.
  46. Mitsogiannis I, Tzelvels L, Dellis A, Issa H, Papatsoris A, Moussa M: **Prostate cancer immunotherapy.** *Expert Opin Biol Ther* 2022, **22**(5):577-590.
  47. Venturini NJ, Drake CG: **Immunotherapy for Prostate Cancer.** *Cold Spring Harb Perspect Med* 2019, **9**(5).
  48. Zhu M, Liu D, Liu G, Zhang M, Pan F: **Caspase-Linked Programmed Cell Death in Prostate Cancer: From Apoptosis, Necroptosis, and Pyroptosis to PANoptosis.** *Biomolecules* 2023, **13**(12).
  49. Kulik G: **Personalized prostate cancer therapy based on systems analysis of the apoptosis regulatory network.** *Asian J Androl* 2015, **17**(3):471-474.
  50. Hao Y, Xie F, He J, Gu C, Zhao Y, Luo W, Song X, Shen J, Yu L, Han Z et al: **PLA inhibits TNF- $\alpha$ -induced PANoptosis of prostate cancer cells through metabolic reprogramming.** *Int J Biochem Cell Biol* 2024, **169**:106554.
  51. Yi X, Li J, Zheng X, Xu H, Liao D, Zhang T, Wei Q, Li H, Peng J, Ai J: **Construction of PANoptosis signature: Novel target discovery for prostate cancer immunotherapy.** *Mol Ther Nucleic Acids* 2023, **33**:376-390.
  52. Wang Y, Zhou J, Zhang N, Zhu Y, Zhong Y, Wang Z, Jin H, Wang X: **A Novel Defined PANoptosis-Related miRNA Signature for Predicting the Prognosis and Immune Characteristics in Clear Cell Renal Cell Carcinoma: A miRNA Signature for the Prognosis of ccRCC.** *International journal of molecular sciences* 2023, **24**(11).
  53. Xiao Y, Yu D: **Tumor microenvironment as a therapeutic target in cancer.** *Pharmacology & therapeutics* 2021, **221**:107753.
  54. Shi X, Cheng X, Jiang A, Shi W, Zhu L, Mou W, Glaviano A, Liu Z, Cheng Q, Lin A et al: **Immune Checkpoints in B Cells: Unlocking New Potentials in Cancer Treatment.** *Advanced science (Weinheim, Baden-Wuerttemberg, Germany)* 2024, **11**(47):e2403423.
  55. Peng S, Lin A, Jiang A, Zhang C, Zhang J, Cheng Q, Luo P, Bai Y: **CTLs heterogeneity and plasticity: implications for cancer immunotherapy.** *Molecular cancer* 2024, **23**(1):58.
  56. Liu L, Xie Y, Yang H, Lin A, Dong M, Wang H, Zhang C, Liu Z, Cheng Q, Zhang J et al: **HPVTIMER: A shiny web application for tumor immune estimation in human papillomavirus-associated cancers.** *iMeta* 2023, **2**(3):e130.
  57. Kainulainen K, Niskanen EA, Kinnunen J, Mäki-Mantila K, Hartikainen K, Paakinaho V, Malinen M, Ketola K, Pasonen-Seppänen S: **Secreted factors from M1 macrophages drive prostate**

- cancer stem cell plasticity by upregulating NANOG, SOX2, and CD44 through NFκB-signaling. *Oncoimmunology* 2024, **13**(1):2393442.
58. Gu Q, Qi A, Wang N, Zhou Z, Zhou X: **Macrophage dynamics in prostate cancer: Molecular to therapeutic insights.** *Biomedicine & pharmacotherapy = Biomedecine & pharmacotherapie* 2024, **177**:117002.
59. Sierra-Filardi E, Nieto C, Domínguez-Soto A, Barroso R, Sánchez-Mateos P, Puig-Kroger A, López-Bravo M, Joven J, Ardavín C, Rodríguez-Fernández JL *et al*: **CCL2 shapes macrophage polarization by GM-CSF and M-CSF: identification of CCL2/CCR2-dependent gene expression profile.** *Journal of immunology (Baltimore, Md : 1950)* 2014, **192**(8):3858-3867.
60. Caescu CI, Guo X, Tesfa L, Bhagat TD, Verma A, Zheng D, Stanley ER: **Colony stimulating factor-1 receptor signaling networks inhibit mouse macrophage inflammatory responses by induction of microRNA-21.** *Blood* 2015, **125**(8):e1-13.
61. Yi-Hong C, Jing L, Lu H: **[MicroRNA-155 induces macrophage polarization to M1 in Toxoplasma gon-dii infection].** *Zhongguo xue xi chong bing fang zhi za zhi = Chinese journal of schistosomiasis control* 2019, **30**(6):652-655.
62. Fei Y, Wang Z, Huang M, Wu X, Hu F, Zhu J, Yu Y, Shen H, Wu Y, Xie G *et al*: **MiR-155 regulates M2 polarization of hepatitis B virus-infected tumour-associated macrophages which in turn regulates the malignant progression of hepatocellular carcinoma.** *Journal of viral hepatitis* 2023, **30**(5):417-426.
63. Nicholson DW: **Caspase structure, proteolytic substrates, and function during apoptotic cell death.** *Cell death and differentiation* 1999, **6**(11):1028-1042.
64. Lamkanfi M, Kanneganti TD: **Caspase-7: a protease involved in apoptosis and inflammation.** *The international journal of biochemistry & cell biology* 2010, **42**(1):21-24.
65. Kim SH, Baek KH: **Ovarian tumor deubiquitinase 6A regulates cell proliferation via deubiquitination of nucleolin and caspase-7.** *International journal of oncology* 2022, **61**(4).
66. Nishikura K: **Functions and regulation of RNA editing by ADAR deaminases.** *Annual review of biochemistry* 2010, **79**:321-349.
67. Ramírez-Moya J, Miliotis C, Baker AR, Gregory RI, Slack FJ, Santisteban P: **An ADAR1-dependent RNA editing event in the cyclin-dependent kinase CDK13 promotes thyroid cancer hallmarks.** *Molecular cancer* 2021, **20**(1):115.
68. Yu H, Bai K, Cheng Y, Lv J, Song Q, Yang H, Lu Q, Yang X: **Clinical significance, tumor immune landscape and immunotherapy responses of ADAR in pan-cancer and its association with proliferation and metastasis of bladder cancer.** *Aging* 2023, **15**(13):6302-6330.
69. Qian W, Wang J, Van Houten B: **The role of dynamin-related protein 1 in cancer growth: a promising therapeutic target?** *Expert opinion on therapeutic targets* 2013, **17**(9):997-1001.
70. Inoue-Yamauchi A, Oda H: **Depletion of mitochondrial fission factor DRP1 causes increased apoptosis in human colon cancer cells.** *Biochemical and biophysical research communications* 2012, **421**(1):81-85.
71. Xie Q, Wu Q, Horbinski CM, Flavahan WA, Yang K, Zhou W, Dombrowski SM, Huang Z, Fang X, Shi Y *et al*: **Mitochondrial control by DRP1 in brain tumor initiating cells.** *Nature neuroscience* 2015, **18**(4):501-510.
72. Liston P, Roy N, Tamai K, Lefebvre C, Baird S, Cherton-Horvat G, Farahani R, McLean M, Ikeda JE, MacKenzie A *et al*: **Suppression of apoptosis in mammalian cells by NAIP and a related family of IAP genes.** *Nature* 1996, **379**(6563):349-353.

73. Martinon F, Tschopp J: **Inflammatory caspases and inflammasomes: master switches of inflammation.** *Cell death and differentiation* 2007, **14**(1):10-22.
74. Chen YK, Huse SS, Lin LM: **Expression of inhibitor of apoptosis family proteins in human oral squamous cell carcinogenesis.** *Head & neck* 2011, **33**(7):985-998.
75. Choi J, Hwang YK, Choi YJ, Yoo KE, Kim JH, Nam SJ, Yang JH, Lee SJ, Yoo KH, Sung KW *et al*: **Neuronal apoptosis inhibitory protein is overexpressed in patients with unfavorable prognostic factors in breast cancer.** *Journal of Korean medical science* 2007, **22** Suppl(Suppl):S17-23.

## TABLES AND FIGURES WITH LEGENDS

**Table 1.**

Gene	Target sequences (5'-3')
si-ADAR-1	CAGTAGTTTCCTGCTTAAGCAA
si-ADAR-2	CTGCGACTATCTCTTCAATGTGT

**Table 2.**

Gene	Forward primer sequence (5'-3')	Reverse primer sequence (5'-3')
------	---------------------------------	---------------------------------

<i>CASP7</i>	CGGAACAGACAAAGATGCCG AG	AGGCGGCATTTGTATGGTCCT C
<i>ADAR</i>	TCCGTCTCCTGTCCAAAGAAG G	TTCTTGCTGGGAGCACTCACA C
<i>DNMI</i> <i>L</i>	GATGCCATAGTTGAAGTGGTG AC	CCACAAGCATCAGCAAAGTC TGG
<i>NAIP</i>	CCGAACAGGAACTGCTTCTCA C	CCACAGACAGTTCTTTCAGGC AC
<i>CDH1</i>	GCCTCCTGAAAAGAGAGTGG AAG	TGGCAGTGTCTCTCCAAATCC G
<i>CDH2</i>	CCTCCAGAGTTTACTGCCATG AC	GTAGGATCTCCGCCACTGATT C
<i>VIM</i>	AGGCAAAGCAGGAGTCCACT GA	ATCTGGCGTTCCAGGGACTCA T
<i>BAX</i>	TCAGGATGCGTCCACCAAGAA G	TGTGTCCACGGCGGCAATCAT C
<i>CASP1</i>	GCTGAGGTTGACATCACAGGC A	TGCTGTCAGAGGTCTTGTGCT C
<i>GSDM</i> <i>D</i>	ATGAGGTGCCTCCACAACCTC C	CCAGTTCCTTGGAGATGGTCT C
<i>GAPD</i> <i>H</i>	GTCTCCTCTGACTTCAACAGC G	ACCACCCTGTTGCTGTAGCCA A

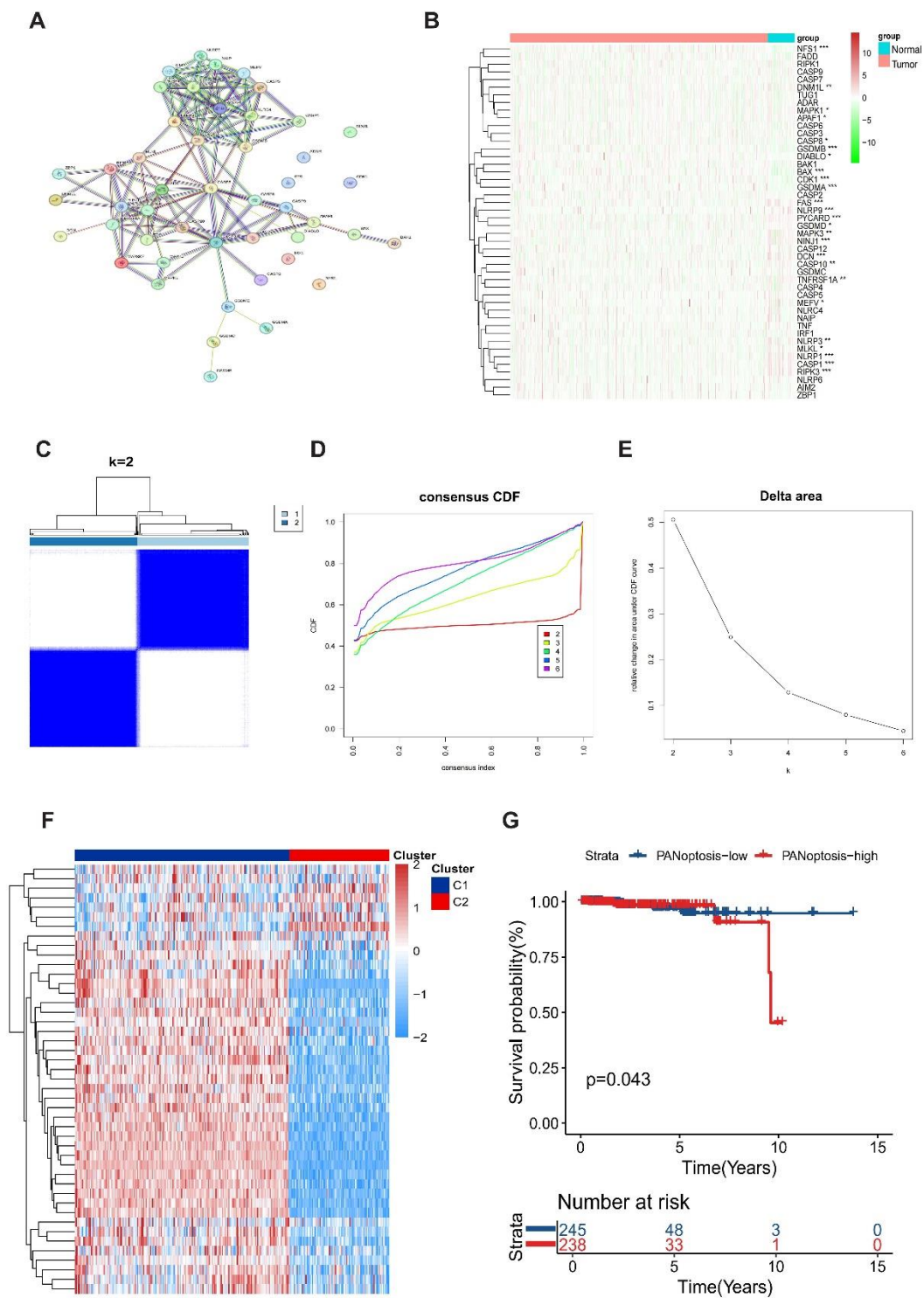


**Figure 1. Identification of PANoptosis-associated subtypes. (A)** The interactions

between proteins encoded by PANoptosis-associated genes; (B) The heatmap illustrates consensus clustering, presenting the expression profiles of 45 PANoptosis-associated genes in normal and PCa samples within the TCGA database; (C) Consensus clustering results ( $k = 2$ ) displayed as a heatmap for 45 genes in PCa specimens; (E) Delta area plot for consensus clustering showing area changes under the CDF curve from  $k = 2$  through 6; (F) Expression distribution of 45 PRGs across diverse subtypes depicted in a heatmap, where red denotes elevated expression and blue indicates reduced expression; (G) OS analysis using KM curves comparing PANoptosis-high versus PANoptosis-low groups.  $*P < 0.05$ ,  $**P < 0.01$ ,  $***P < 0.001$ , &  $****P < 0.0001$ .

EARLY ACCESS

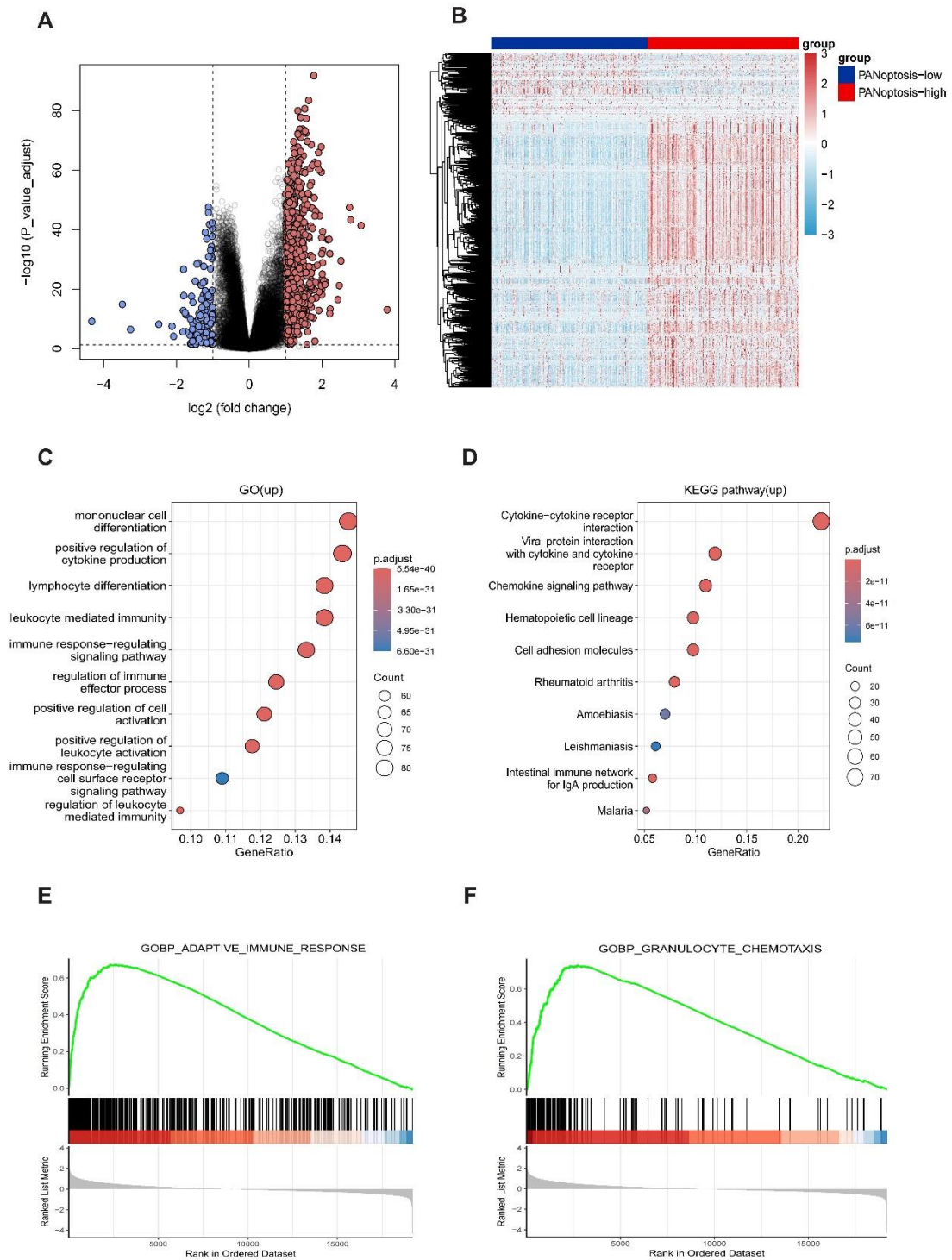


**Figure 2. Identification of DEGs and associated signaling cascades across subgroups.** (A) A volcano plot demonstrates DEG distribution, obtained through comparison between PANoptosis-high versus PANoptosis-low subtypes, utilizing thresholds of  $|\log_2 \text{Fold change}| > 1$  and  $p.\text{adjust-value} < 0.05$  within the TCGA cohort;

(B) Expression patterns of DEGs among various subtypes are illustrated through a heatmap; (C) Pathway enrichment examination of KEGG and GO signals is shown via dot plot, where dot dimensions reflect gene quantities and color intensity indicates p.adjust-value; (D) Pathway distinction between PANoptosis-high and PANoptosis-low subtypes is revealed through GSEA evaluation.

EARLY ACCESS

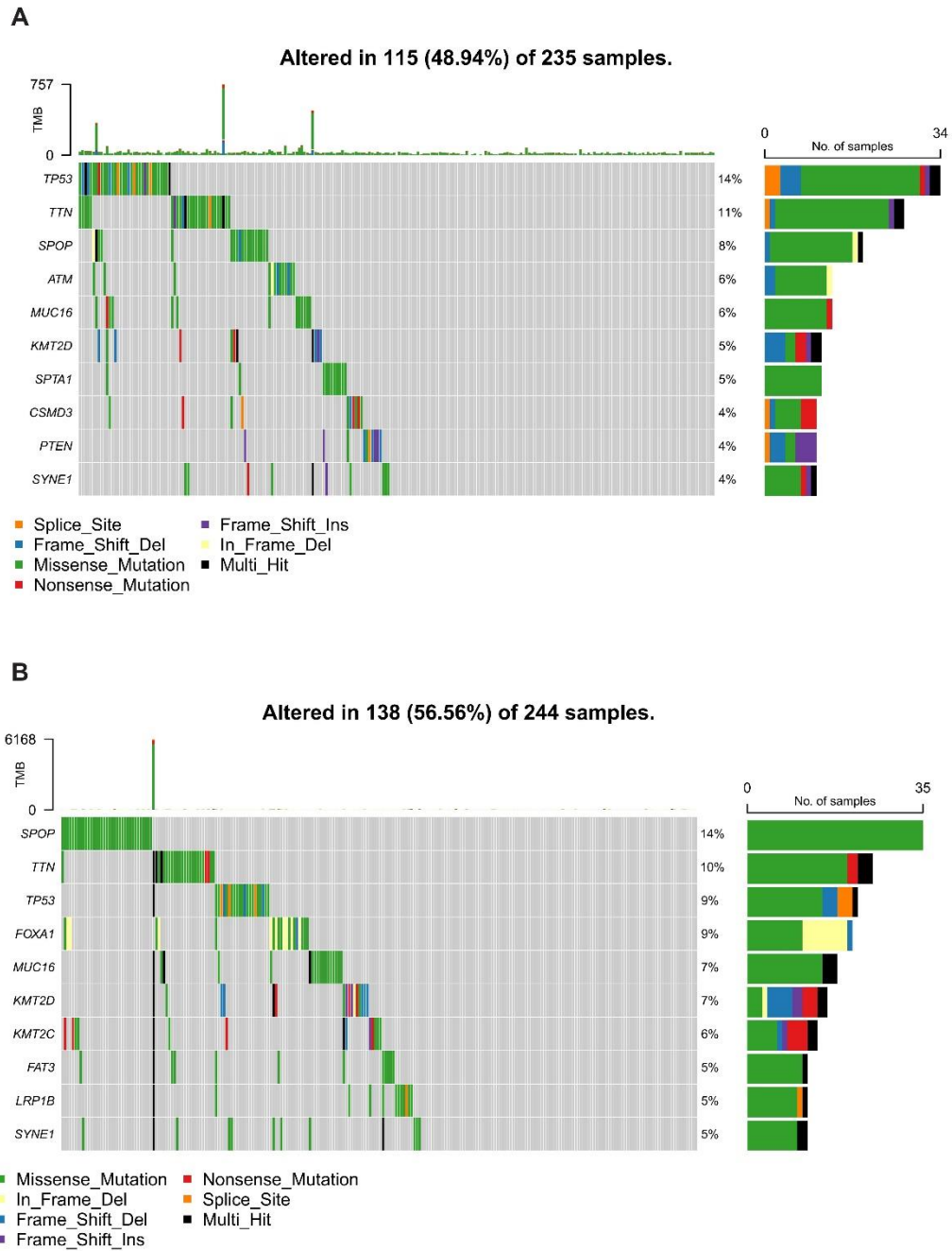


**Figure 3. Analysis of somatic alterations across distinct PANoptosis subtypes. (A, B) Graphical representation displaying the top ten genes with the highest mutation frequencies in PANoptosis-high (A) and PANoptosis-low (B) subtypes.**

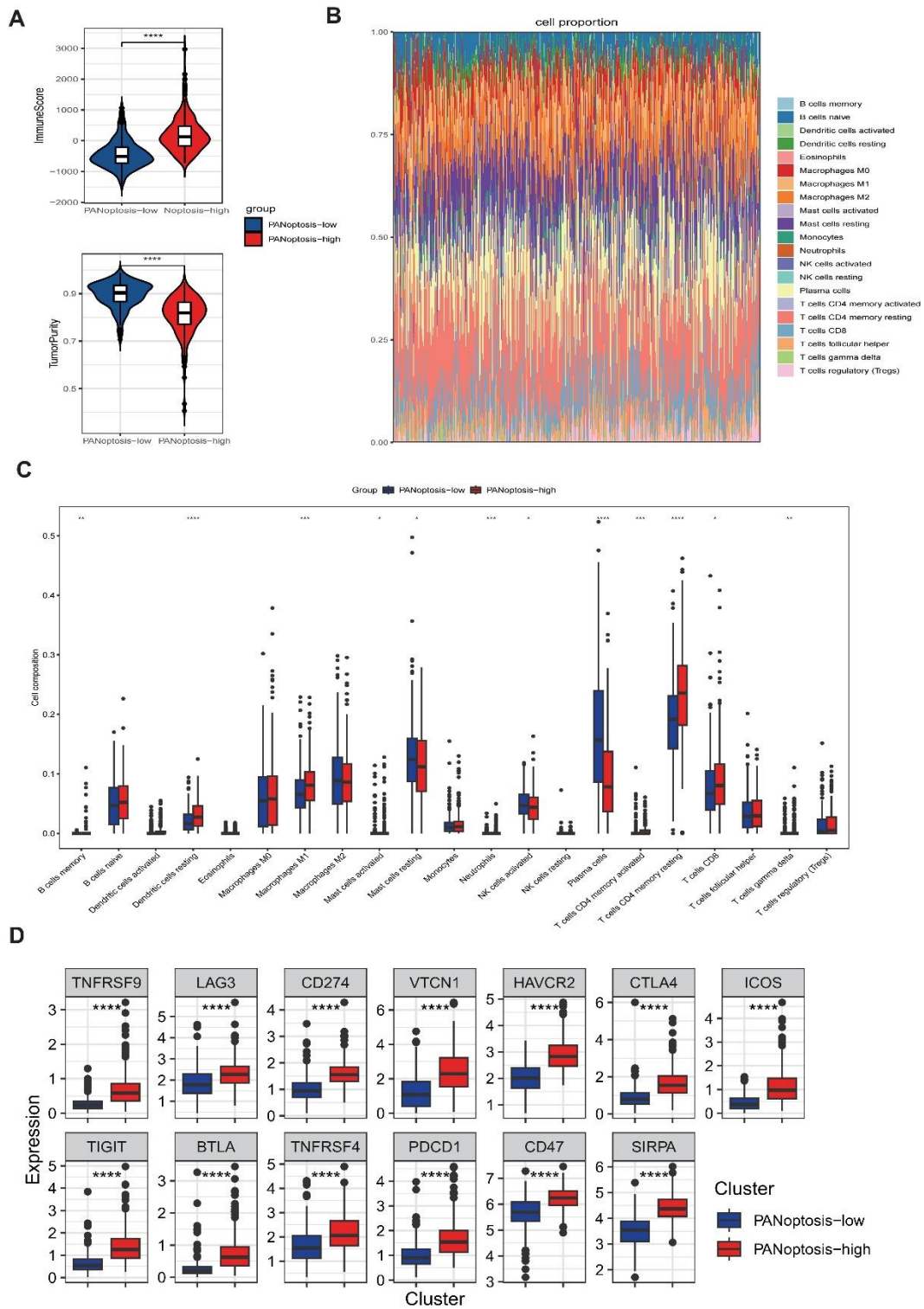


**Figure 4. Immune landscape of PANoptosis-high and PANoptosis-low subtypes.** (A) Violin plots depict the median and quartile estimations for each immune score, along with the tumor purity score; (B) Relative proportions of immune infiltration across subtypes; (C) Violin plots illustrate notable variations in immune cell composition

between subtypes; (D) Box plots display the differential expression of multiple immune checkpoints in PANoptosis-high and PANoptosis-low subtypes. \* $P < 0.05$ , \*\* $P < 0.01$ , \*\*\* $P < 0.001$ , & \*\*\*\* $P < 0.0001$ .

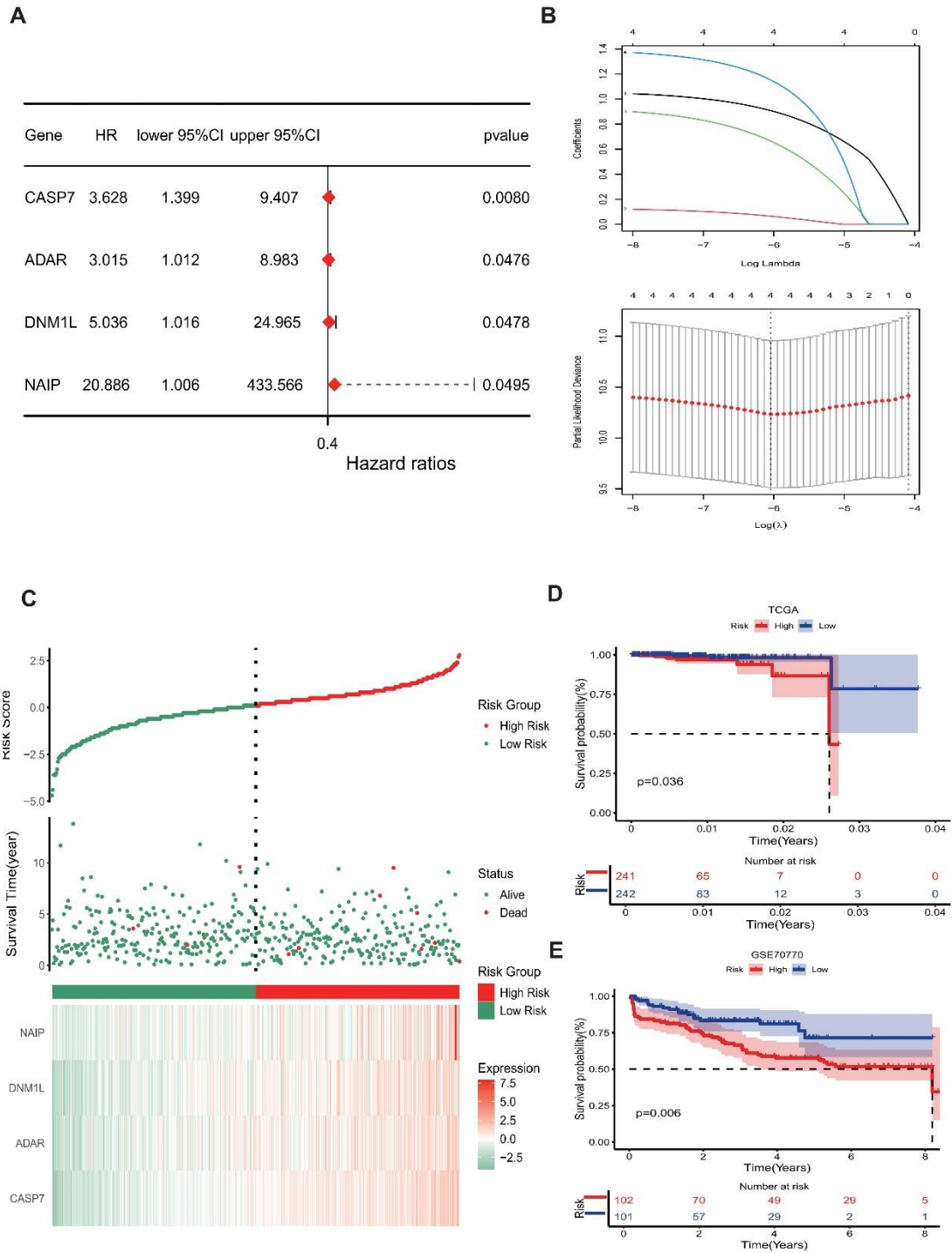


**Figure 5. Construction and validation of the PANoptosis risk signature.** (A) The

prognostic value of PANoptosis-related genes concerning OS is assessed through univariate Cox analysis; (B) Lasso-Cox regression identifies four genes most closely linked to OS in the TCGA dataset; (C) The distribution of risk scores, patient survival status, and heatmaps representing the prognostic four-gene signature within the TCGA database; (D, E) KM analyses illustrate the prognostic relevance of the risk model in the TCGA and GSE70770 cohorts.

EARLY ACCESS

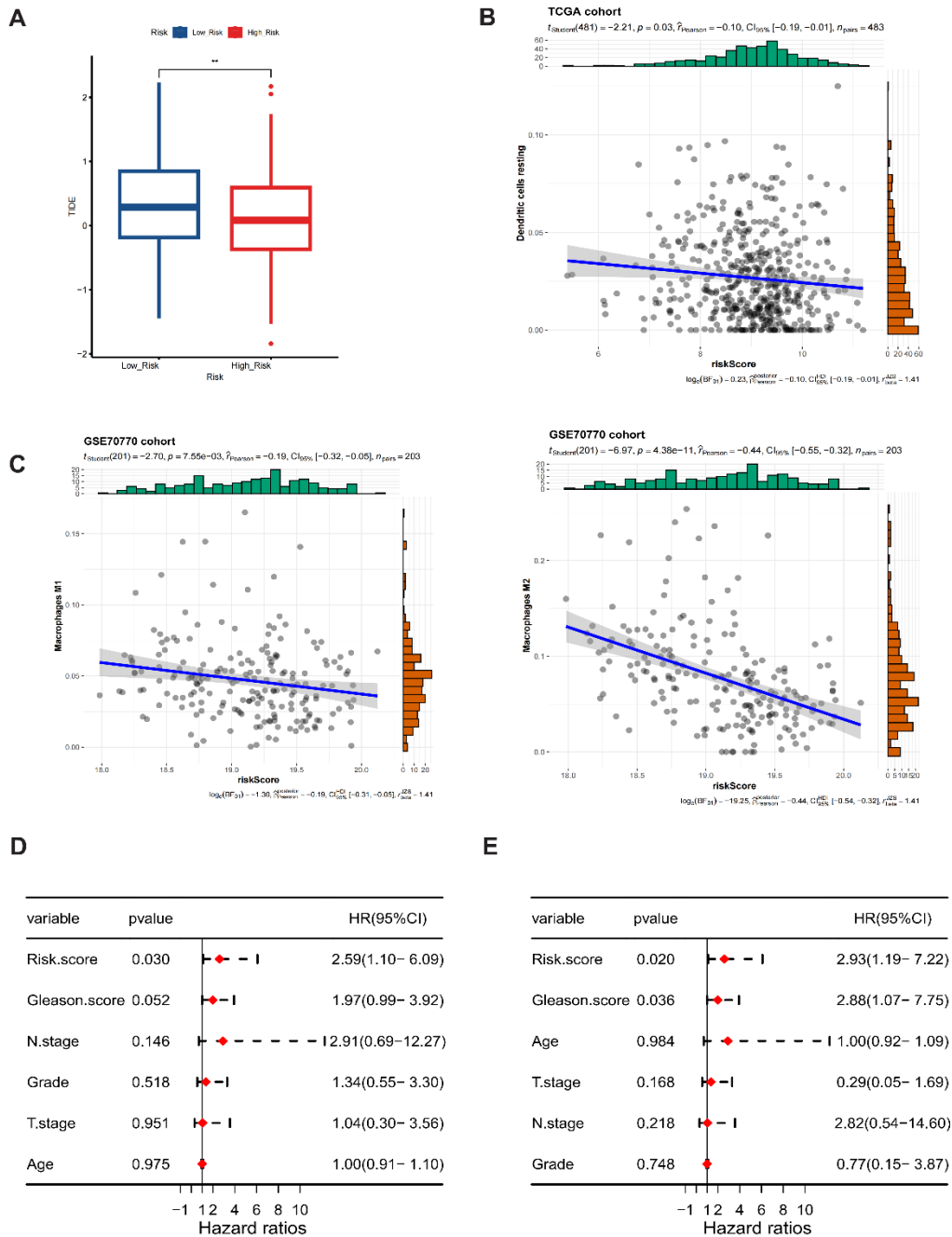


**Figure 6. Association between the PANoptosis risk signature and the TME. (A, B)** Scatter plots illustrate the correlation between the risk score and immune cell infiltration within the TCGA cohort (A), further validated in the GSE70770 cohort (B); (C) The box plot depicts the link between the PANoptosis risk score and

immunotherapy response; (D, E) Univariate and multivariate Cox analyses assess the independent prognostic significance of the PANoptosis risk signature in individuals with PCa.

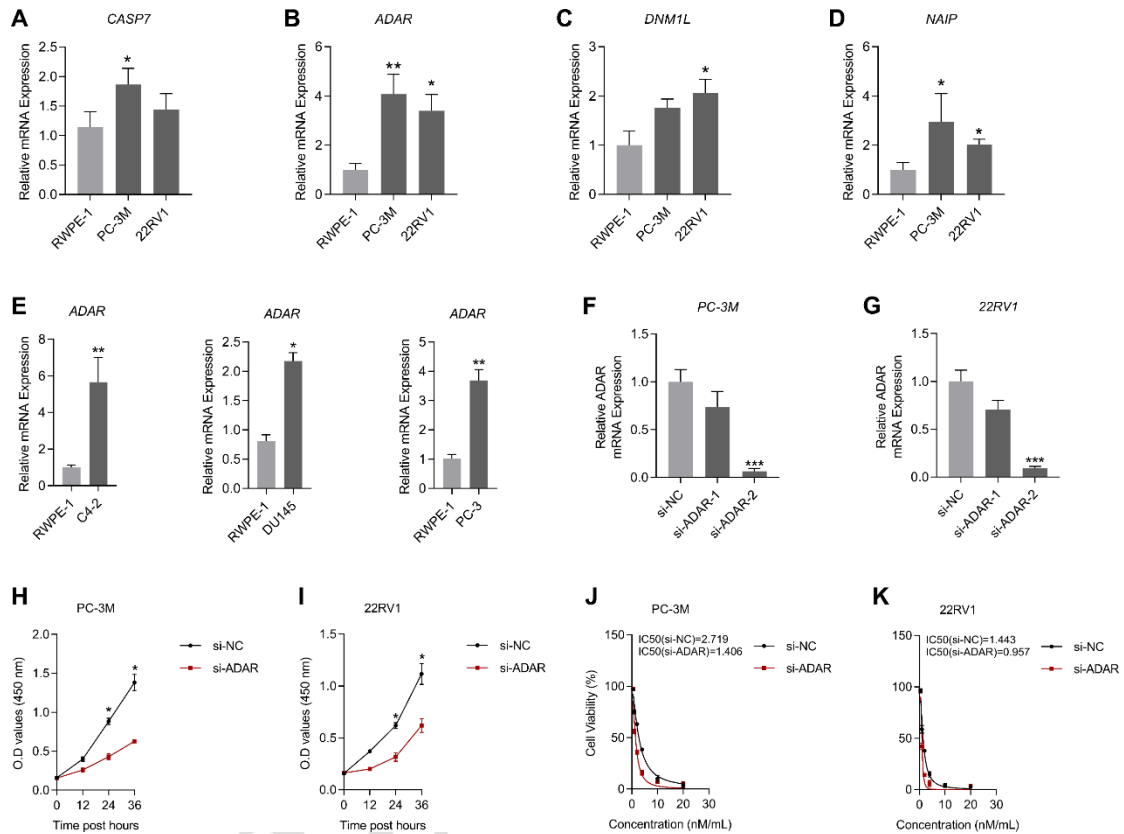


**Figure 7. ADAR is upregulated in PCa cell lines.** (A-D) The transcript levels of CASP7, ADAR, DNMT1L, and NAIP were analyzed through qRT-PCR in RWPE-1, PC-3M, and 22RV1 cell lines; (E) qRT-PCR was conducted to assess ADAR transcript levels in RWPE-1, C4-2, DU145, and PC-3 cell lines; (F-G) The knockdown efficiency of small interfering RNAs targeting ADAR in PC-3M and 22RV1 was evaluated by qRT-PCR; (H-I) Changes in PC-3M and 22RV1 cell viability before and after ADAR silencing were observed; (J-K) IC50 variations in PC-3M and 22RV1 following treatment with Docetaxel before and after ADAR knockdown. n=3/per cohort.

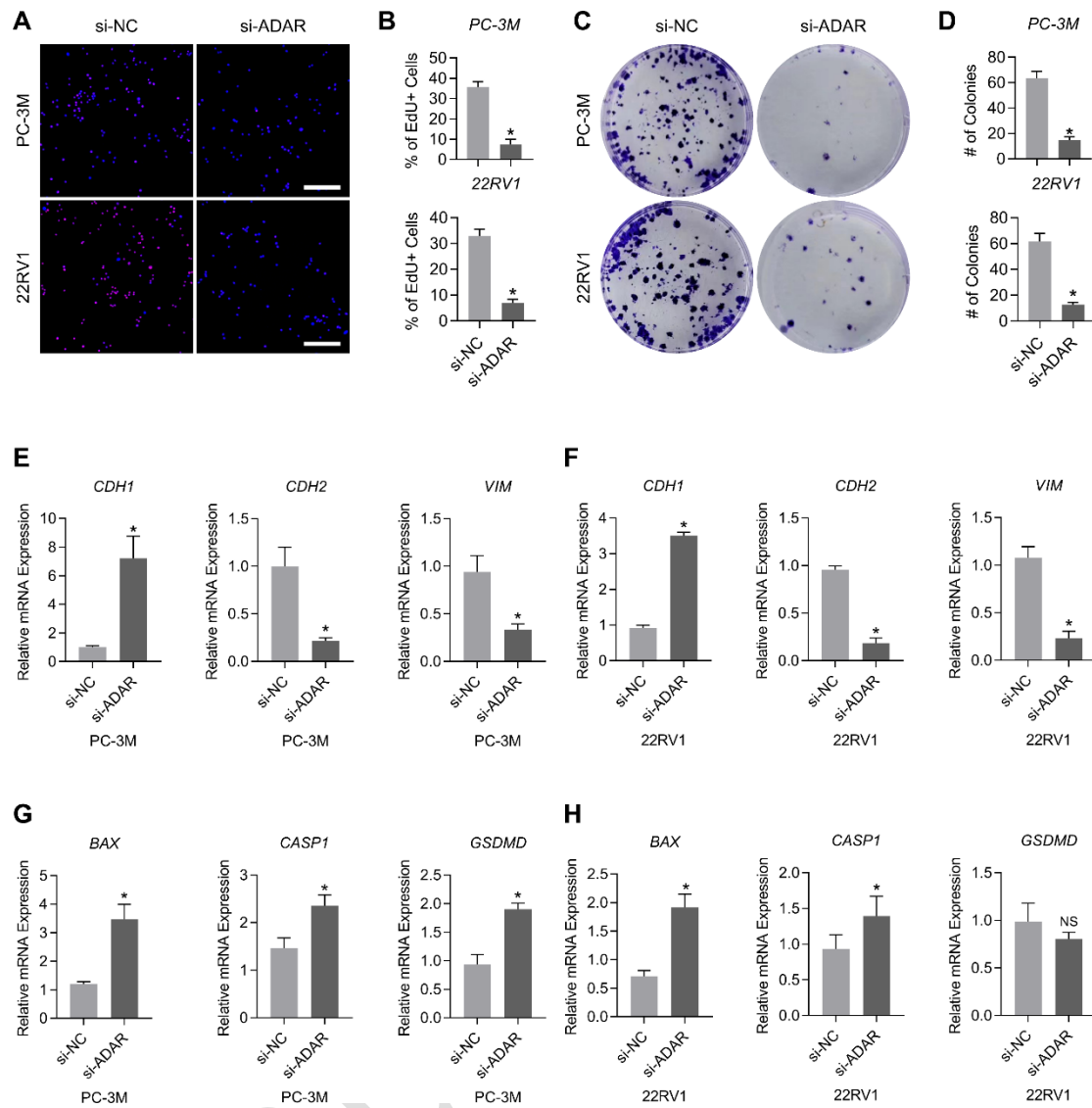


**Figure 8. ADAR promotes PCa progression *in vitro*.** (A-B) Variations in the proportion of EdU-positive cells in PC-3M and 22RV1 before and after ADAR knockdown; (C-D) Changes in clone formation numbers in PC-3M and 22RV1 before and after ADAR knockdown; (E-F) Expression alterations of CDH1, CDH2, and VIM in PC-3M and 22RV1 before and after ADAR knockdown; (G-H) Modifications in the expression of BAX, CASP1, and GSDMD in PC-3M and 22RV1 following ADAR knockdown. n=3/per cohort.

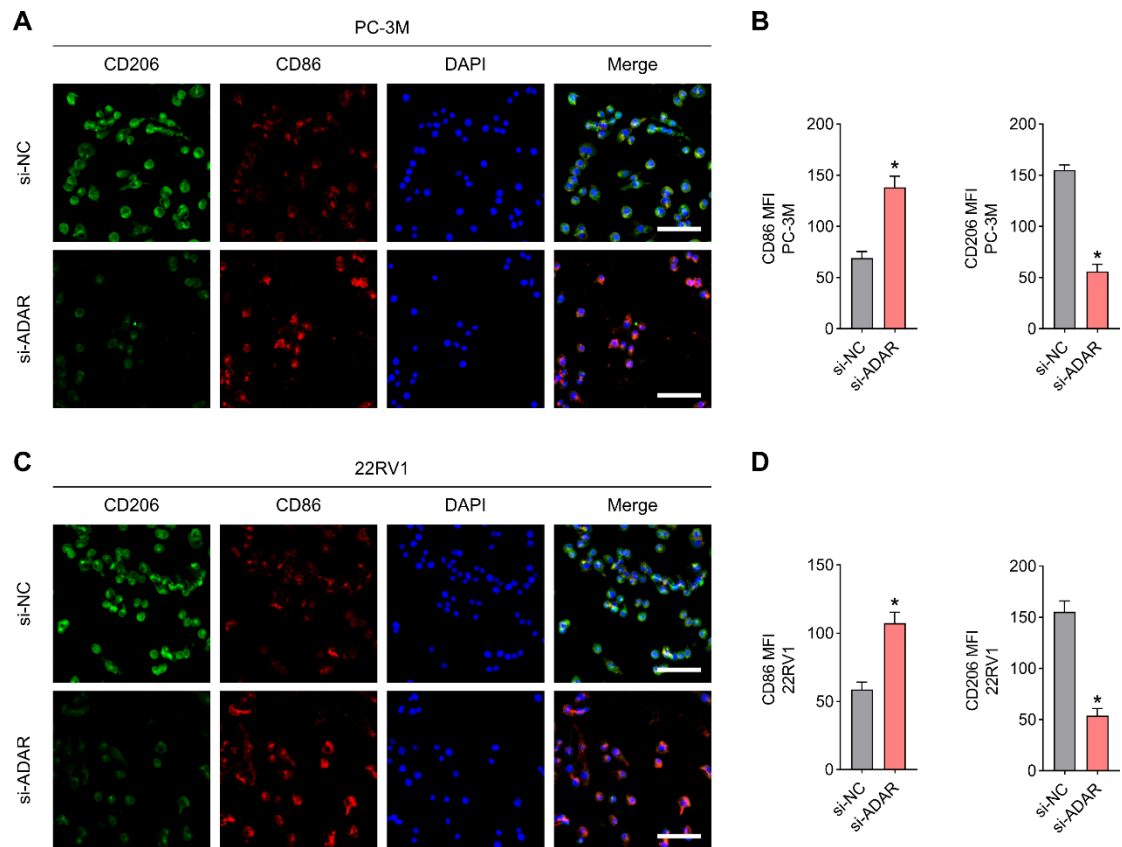


**Figure 9. ADAR modulates macrophage polarization.** (A-D) Changes in the surface expression levels of CD86 and CD206 in macrophages before and after ADAR knockdown. n=3/per cohort.

Table S1. List of PANoptosis-related genes.